DEVELOPMENT OF A WALL-TO-FLUID HEAT TRANSFER PACKAGE FOR THE SPACE CODE

KI YONG CHOI*, BYONG JO YUN, HYUN SIK PARK, HEE DONG KIM, YEON SIK KIM, KWON-YEONG LEE and KYUNG DOO KIM
Korea Atomic Energy Research Institute
1045 Daedeokdaero, Yuseong-gu, Daejeon, Korea
*Corresponding author. E-mail : kychoi@kaeri.re.kr

Received February 10, 2009
Accepted May 15, 2009

The SPACE code that is based on a multi-dimensional two-fluid, three-field model is under development for licensing purposes of pressurized water reactors in Korea. Among the participating research and industrial organizations, KAERI is in charge of developing the physical models and correlation packages for the constitutive equations. This paper introduces a developed wall-to-fluid heat transfer package for the SPACE code. The wall-to-fluid heat transfer package consists of twelve heat transfer sub-regions. For each sub-region, the models in the existing safety analysis codes and the leading models in literature have been peer reviewed in order to determine the best models which can easily be applicable to the SPACE code. Hence a wall-to-fluid heat transfer region selection map has been developed according to the non-condensable gas quality, void fraction, degree of subcooling, and wall temperature. Furthermore, a partitioning methodology which can take into account the split heat flux to the continuous liquid, entrained droplet, and vapor fields is proposed to comply fully with the three-field formulation of the SPACE code. The developed wall-to-fluid heat transfer package has been pre-tested by varying the independent parameters within the application range of the selected correlations. The smoothness between two adjacent heat transfer regimes has also been investigated. More detailed verification work on the developed wall-to-fluid heat transfer package will be carried out when the coupling of a hydraulic solver with the constitutive equations is brought to completion.

KEYWORDS : SPACE, System Code, Heat Transfer

1. INTRODUCTION

Korea Hydraulic and Nuclear Power (KHNP) and the Ministry of Commerce and Industry and Energy (MOCIE) have launched a nuclear reactor thermal hydraulics system analysis code development program. The SPACE (Safety and Performance Analysis Code) code, which has a multi-dimensional analysis capability by incorporating a dispersed liquid phase into the thermo-hydraulic field equations, is under development for the safety analysis of PWRs. Several research and industrial organizations are participating in the collaboration for the development program, including KAERI (Korea Atomic Energy Research Institute), KHNP (Korea Hydro & Nuclear Power Co., Ltd.), KOPEC (Korea Power Engineering Company, Inc.), and KNF (Korea Nuclear Fuel Co., Ltd.).

A hydraulic solver module is being developed by KOPEC. The solver is designed to handle a 3-dimensional unstructured grid system and it has the capability to treat a staggered mesh as well as a collocated mesh. Special models such as a critical flow, mixture level tracking, off-take, and ECC mixing models are being developed by KNF. The main task of KAERI is to develop the physical models and correlation packages for the constitutive equations: wall heat transfer package, wall and interfacial friction package, interfacial heat and mass transfer package, entrainment/de-entrainment model package, and flow regime selection package. In addition to that, KAERI is also responsible for carrying out separate effect tests (SET) and integral effect tests (IET) for code verification and validation (V&V). The separate effect tests have the purpose of generating benchmark data for multi-dimensional two-phase phenomena. The detailed test items have been defined. The integral effect tests will be performed with ATLAS (Advanced Thermal-hydraulic Test Loop for Accident Simulation), which is a 1/2 reduced height and 1/288 volume scaled test facility based on the design features of the APR1400. This code development program is being coordinated by KEPRI (Korea Electric Power Research Institute) to consolidate the technology of the participating organizations effectively. Furthermore, a technical consulting committee was constituted from the academic field in order to support the program by performing an independent review on the progress on a regular basis.

This paper describes the development program for a wall-to-fluid heat transfer package for the SPACE code. The developed wall-to-fluid heat transfer package consists of a heat transfer mode transition map, and heat transfer models for each region of the well-known Nukiyama's boiling curve [1]. The wall-to-fluid heat transfer package determines the energy transfer from a heat structure to a calculation cell. Due to the three-field formulation of the SPACE code, the energy transfer from a heat structure should be partitioned into three parts: wall-to-vapor, wall-to-liquid, and wall-to-droplets.

2. WALL-TO-FLUID HEAT TRANSFER PACKAGE

2.1 Development of a Heat Transfer Mode Transition Map

The wall-to-fluid heat transfer mode consists of a liquid phase natural convection, liquid phase forced convection, nucleate boiling, critical heat flux, transition boiling, film boiling, vapor phase convection, and condensation heat transfer. Unfortunately, there is no physical model which can integrate the relevant correlations and form a cohesive model for the Nukiyama's boiling curve. Hence, the wall-to-fluid heat transfer mode should be defined in advance and be classified depending on whether a physical model is available for the defined heat transfer mode. For the SPACE code, a total of 12 heat transfer modes were determined as shown in Table 1. The

Table 1. Classification of the Wall-to-fluid Heat Transfer Modes

Mode	Application
Mode 0	Convection to a non-condensable steam-water mixture
Mode 1	Natural convection to a single phase liquid
Mode 2	Forced convection to a single phase liquid
Mode 3	Subcooled nucleate boiling
Mode 4	Saturated nucleate boiling
Mode 5	Subcooled transition boiling
Mode 6	Saturated transition boiling
Mode 7	Subcooled film boiling
Mode 8	Saturated film boiling
Mode 9	Convection to a single phase vapor
Mode 10	Convection at a supercritical pressure
Mode 11	Condensation

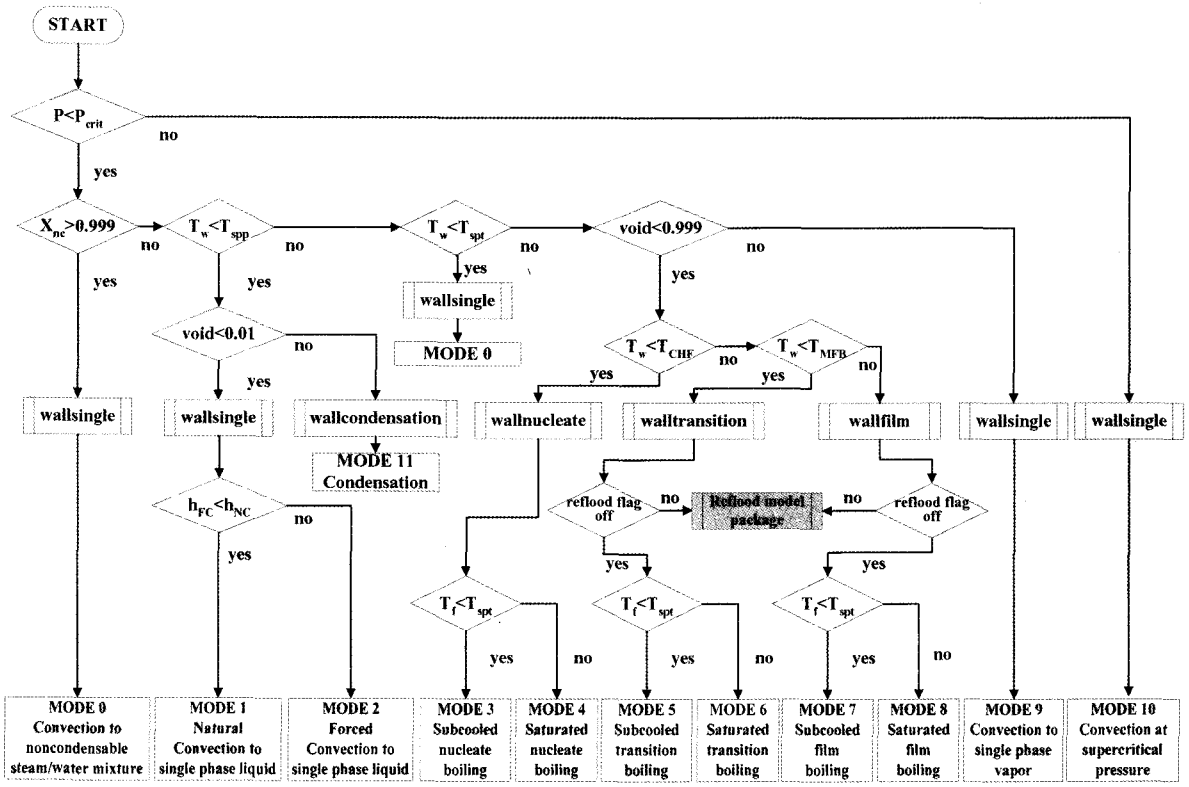

Fig. 1. Heat Transfer Mode Transition Map

classification is mainly based on the physical heat transfer phenomena occurring on a wall contacted by a fluid. In particular, the detailed classification for the subcooled and saturated conditions is to provide the necessary information on the calculation cell to code users.

A heat transfer mode transition map was developed to make sure of a smooth transition between two adjacent heat transfer modes and to minimize any numerical instability. The heat transfer mode transition is based on the pressure, non-condensable gas quality, void fraction, degree of subcooling, and wall temperature. In particular, the minimum film boiling temperature, TMFB, is used to define the boundary between the transition and the film boiling heat transfer modes. The developed heat transfer mode transition map is shown in Fig. 1. At the present stage, only a branch point to the reflood heat transfer mode is included in the present heat transfer mode transition map as a reflood heat transfer package has not been developed yet. Most safety analysis codes such as RELAP5/MOD3.3 and TRAC-M deal with the wall-to-fluid heat transfer under a reflood condition with a separate model package. The separate reflood heat transfer package is incorporated into a heat structure model which takes account of the two-dimensional conduction effects. When the development of the reflood heat transfer package is completed, a reflood heat transfer selection logic will be added to the present heat transfer mode transition map.

2.2 Development of a Heat Transfer Package

In order to select a wall-to-fluid heat transfer model for the SPACE code, the models currently used in major best-estimate nuclear reactor system analysis codes, such as RELAP5, TRAC-M, TRACE, COBRA-TF and CATHARE, have been peer reviewed. Furthermore, an extensive literature survey was conducted in order to choose the best wall-to-fluid heat transfer model which can be applied easily to the SPACE code. Through an in-depth literature review process, the best model for each heat transfer mode was selected and implemented into the SPACE code. In the heat transfer regime in which a model's uncertainty is expected to be high, an alternative model is additionally programmed as a user option. The selected heat transfer models, including the wall-to-fluid heat transfer package of the SPACE code, are summarized in Table 2. A detailed description of the selected model can be found in Kim et al. [2].

Table 2. Heat Transfer Models of Existing Codes

Regimes	Models
Natural convection	McAdams for laminar, Warner & Arpaci for turbulent
Forced convection	Sellars for laminar, Dittus-Boelter for turbulent
Nucleate Boiling	Lahey, Ha, Chen
CHF	1) 2006 AECL-UO look-up table, 2) Biasi
Transition Boiling	1) Chen, 2) Bjornard, 3) Jones, 4) Elias, 5) TRACE
Film Boiling	1) 2004 AECL-UO look-up table, 2) Bromley
Condensation	pure steam : max (Nusselt, Chato, Shah) mixture : 1) Colburn-Hougen 2) Non-iterative model (No-Park)

2.2.1 Heat Flux Partitioning

In the SPACE code, the wall heat flux transmitted to one of three fields is generally formulated by the sum of the heat flux components based on three possible reference temperatures. The general expression for the total wall heat flux can be written as

$$q''_{total} = q''_l + q''_d + q''_v = \sum_{k=l,d,v} \left[h_{kk}(T_w - T_k) + h_{kt}(T_w - T_{spt}) + h_{kp}(T_w - T_{spp}) \right] \quad (1)$$

where the subscript index k can be either l, d, or v for continuous liquid, dispersed droplet, or vapor, respectively. The subscript kk indicates the heat transfer coefficient to the phase k, with the phase temperature as the reference temperature; kt indicates the heat transfer coefficient to the phase k, with the saturation temperature based on the total pressure T_{spt} as the reference temperature; and kp indicates the heat transfer coefficient to the phase k, with the saturation temperature based on the vapor partial pressure T_{spp} as the reference temperature. T_w and T_k indicate wall temperature and phase temperature, respectively. The total wall heat flux in Eq. (1) is used as a convective boundary condition of the conduction equation, which ultimately calculates the wall temperature of the solid heat structure. Only some of the heat transfer coefficients are nonzero in most heat transfer regimes.

2.2.2 Natural Convection

It is found that the natural circulation models used in the TRAC-M code are the best from an extensive literature survey. The McAdams' model [3] and Warner & Arpaci's model [4] were selected for the SPACE code for the conditions of a laminar and a turbulent flow, respectively.

- laminar flow (McAdams' model)

$$h = 0.59 \frac{k_l}{D_h} (Gr \cdot \Pr)^{1/4} \quad \text{for} \quad 10^4 < (Gr \cdot \Pr) < 10^9 \quad (2)$$

- turbulent flow (Warner & Arpaci's model)

$$h = 0.10 \frac{k_l}{D_h} (Gr \cdot \Pr)^{0.3333} \quad \text{for} \quad 10^9 < (Gr \cdot \Pr) < 10^{13} \quad (3)$$

where k_l indicates conductivity of the liquid phase and D_h indicates a heated equivalent diameter of the calculation cell. Gr and Pr is the Grashof number and Prandtl number, respectively.

2.2.3 Forced Convection

In the case of a forced convection, the well-known Dittus-Boelter correlation [5] was selected as a default model for the SPACE code for the condition of a turbulent flow. This correlation is based on a broad range of experimental data obtained from a smooth tube and it is widely used in the existing safety analysis codes. Though simple, it is known that its prediction accuracy is excellent for an application to other geometric conditions and single phase gas flow conditions as well. Moreover, the Gnielinski correlation [6] was selected as an alternative model for the condition of a turbulent flow. For the laminar forced convection flow, Sellars' analytical solution [7] was used for the SPACE code. A variation of the correlations for other geometries rather than a round tube was not taken into account in the SPACE code in the present phase. Such geometric effects will be considered and will be implemented during the verification and validation phase if necessary.

- laminar flow (Sellars' model)

$$h = 4.36\frac{k_l}{D_h} \qquad \text{for Re} < 2300 \qquad (4)$$

- turbulent flow (default: Dittus-Boelter correlation)

$$h = 0.023 \cdot \text{Re}^{0.8} \cdot \text{Pr}^{0.4} \qquad \text{for Re} > 2300 \qquad (5)$$

- turbulent flow (alternative: Gnielinski correlation)

$$Nu = \frac{(\text{Re}-1000)\cdot \text{Pr}\cdot f/8}{1.0+12.7(\text{Pr}^{2/3}-1)\sqrt{f/8}} \qquad \text{for Re} > 2300 \qquad (6)$$

where

$$f = (1.82\log \text{Re} - 1.64)^{-2}$$

The SPACE code evaluates both a natural convection and a forced convection heat transfer coefficient and takes the maximum value as a final heat transfer coefficient. In the case of a forced convection heat transfer mode to a single phase liquid (mode 2), the obtained final heat transfer coefficient is equal to h_{ll} and the other heat transfer coefficients in Eq. (1) become zero. On the other hand, for the forced convection heat transfer mode to a single phase vapor (mode 9), the calculated heat transfer coefficient becomes h_{vv} and the other heat transfer coefficients in Eq. (1) are zero.

2.2.4 Nucleate Boiling

The nucleate boiling model consists of a subcooled nucleate boiling model and a saturated nucleate boiling model. The subcooled nucleate boiling model is composed of a net vapor generation model (NVG), a subcooled heat transfer coefficient model, and a pumping model. For the subcooled nucleate boiling model, Lahey's model [8] was selected because its prediction accuracy and numerical stability are widely accepted in this technical field. The accuracy of the void fraction under a subcooled nucleate boiling greatly depends on the NVG model. Lahey's model includes the NVG model proposed by Saha and Zuber [9]. Recently, Ha [10] modified Saha and Zuber's NVG model in order to improve its prediction accuracy in low pressure conditions.

$$h_{cr} = h_{f,sat} - \frac{St \cdot Pe^{0.124} C_{pf}}{0.0287} \qquad \text{for} \quad Pe > 52000 \qquad (7)$$

$$h_{cr} = h_{f,sat} - \frac{St \cdot Pe^{.08} C_{pf}}{918.525} \qquad \text{for} \quad Pe \le 52000 \qquad (8)$$

where $h_{f,sat}$ and C_{pf} indicate enthalpy and specific heat for saturated water, respectively. St and Pe indicate Stanton number and Peclet number, respectively. Hence, Ha's model is incorporated into Lahey's model as a subcooled nucleate boiling model for the SPACE code. A modified Chen's model [11] was used to obtain the subcooled heat transfer coefficient. This modeling approach is the same as that widely used in the existing safety analysis codes. For the saturated nucleate boiling, Chen's [11] saturated nucleate boiling model was adopted for the SPACE code because it is judged to be the best model. The total heat flux due to nucleation boiling can be expressed in the SPACE code as follows:

$$q''_{total} = h_{mac}(T_w - T_l)\cdot F + h_{mic}(T_w - T_{spt})\cdot S. \qquad (9)$$

where h_{mac} and h_{mic} indicate a macroscopic and a microscopic heat transfer coefficient, respectively. F and S are a Reynolds number factor and a suppression factor, respectively. The macroscopic heat transfer coefficient is calculated from the convective heat transfer correlation and the microscopic heat transfer coefficient is from Chen's model.

In a nucleate boiling heat transfer, the heat flux to the

dispersed droplet and to the vapor field can be assumed to be zero so that the total heat flux is transmitted to the continuous liquid field only. Therefore, only two heat transfer coefficients in Eq. (1) are nonzero and the other heat transfer coefficients become zero, that is, h_{ll} is equal to $h_{mac}\cdot F$ and h_{lt} is equal to $h_{mic}\cdot S$ from Chen's correlation.

In addition, a heat flux for the vapor generation rate calculation is calculated by partitioning the total heat flux with the NVG model suggested by Ha [10] as follows:

$$q''_{total} = q''_{total}\cdot\frac{h_{f,sat}-h_f}{h_{f,sat}-h_{cr}} + q''_{total}\cdot\frac{h_f-h_{cr}}{h_{f,sat}-h_{cr}} \quad \text{if } h_f \geq h_{cr} \tag{10}$$

where the first term on the right hand side indicates the heat flux used for increasing sensible heat of the continuous liquid due to convection and the second term does the heat flux used for boiling. Therefore, the second term on the right hand side is used to calculate the vapor generation rate. If $h_f < h_{cr}$, the vapor generation rate becomes zero and the total heat flux is used for increasing sensible heat of continuous liquid.

2.2.5 Critical Heat Flux

An accurate prediction of the critical heat flux is essential for the wall-to-fluid heat transfer package to be reliable. Most safety analysis codes such as RELAP5/MOD3.3 and CATHARE use the look-up table method proposed by Groeneveld et al. [12] because the look-up table method has several advantages: (a) it has a greater accuracy, (b) it has a wide range of applications, (c) it has a correct asymptotic trend, (d) it requires less computing time, and (e) it can be updated if additional data become available. Meanwhile, Biasi's correlation [13] is also widely used in safety analysis codes such as COBRA-TR and TRAC-M due to its simple functional form. It was used in the old version of the RELAP5/MOD2 code and then it was replaced by the look-up table method in the RELAP5/MOD3 code and its later series because Biasi's correlation over-predicts critical heat flux in a medium range of mass flux. In general, Biasi's correlation is known to have a narrower application range than the look-up table method. Subsequently, the look-up table recently released by Groeneveld et al. [14] is selected for the SPACE code because this look-up table has been intensively assessed by several investigators and continuously improved during the past years. In general, the tube CHF look-up table has been widely applied to bundle geometries. In a bundle or subchannel geometry, the tube CHF look-up table needs to be modified to account for bundle-specific effects. The following eight correction factors which were provided by Groeneveld et al. [15] are implemented into the SPACE code to obtain a bundle CHF.

$$CHF_{bundle} = CHF_{table}(P,G,X)\times k_1\times k_2\times k_3\times k_4\times k_5\times k_6\times k_7\times k_8 . \tag{11}$$

This formulation is based on the assumption that all the correction factors are independent. The detailed form of the bundle correction factors are summarized in Table 3. The eight correction factors have been programmed into the SPACE code.

Heat flux partitioning of the obtained critical heat flux was also taken into account. The CHF from Eq. (11) was transmitted to the continuous liquid field only because the critical heat flux is a physical upper limit of the nucleate boiling heat transfer. The other heat fluxes to the dispersed droplet and the vapor fields can be assumed to be negligible without loss of a physical basis as follows:

$$q''_{CHF,l} = q''_{CHF} = h_{ll}(T_w - T_l) + h_{lt}(T_w - T_{spt}) . \tag{12}$$

$$q''_{CHF,d} = 0.0 . \tag{13}$$

Table 3. Summary of the Correction Factors Applicable to CHF Look-up Table

Factors	Form
K_1, subchannel or tube diameter cross section geometry factor	for $3<D_h<25mm$ $K_1=(0.008/D_h)^{0.5}$ for $D_h>25mm$ $K_1=0.57$
K_2, bundle correction factor	$K_2=\min\left(1.0,\left(\frac{1}{2}+\frac{2\delta}{d}\right)\exp\left(\frac{-x^{1/3}}{2}\right)\right)$
K_3, mid-plane spacer factor for 37-element bundle	$K_3=1+A\exp(-BL_{sp}/D_h)$ $A=1.5K^{0.5}(G/1000)^{0.2}$ $B=0.10$
K_4, heated length factor	for $L/D_h>5$ $K_4=\exp[(D_h/L)\exp(2\alpha_h)$ $\alpha_h=X\rho_f/[X\rho_f+(1-X)\rho_g]$
K_5, axial flux distribution factor	for $X\leq 0$ $K_5=1.0$ for $X>0$ $K_5=q_{loc}/q_{BLA}$
K_6, radial flux distribution factor	for $X\leq 0$ $K_6=q(z)_{avg}/q(z)_{max}$ for $X>0$ $K_6=1.0$
K_7, flow orientation factor	$K_7=1-\exp(-(T_1/3)^{0.5})$ $T_1=\left(\frac{1-X}{1-\alpha}\right)^2\frac{f_f G^2}{gD_h\rho_f(\rho_f-\rho_g)\alpha^{0.5}}$
K_8, vertical low flow factor	$G<-400kg\cdot m^{-2}\cdot s^{-1}$ or $X<<0$ $K_8=1.0$ $-400<G<0\ kg\cdot m^{-2}\cdot s^{-1}$ $CHF=CHF_{G=0,X=0}(1-\alpha_h)C_1$ for $\alpha_h<0.8$ $C_1=1.0$ for $\alpha_h>0.8$ $C_1=\frac{0.8+0.2\rho_f/\rho_g}{\alpha_h+(1-\alpha_h)\rho_f/\rho_g}$

$$q''_{CHF,v} = 0.0. \quad (14)$$

For a determined CHF from the look-up table method, Eq. (9) is solved implicitly to obtain a wall temperature at a CHF point which is used as an important reference temperature to determine the boundary between the pre-CHF and the post-CHF heat transfer regime. Once Eq. (9) is solved successfully for a given heat flux, the critical heat flux can easily be partitioned into two parts based on the two possible reference temperatures as shown in Eq. (12). Hence, only two heat transfer coefficients, h_{ll} and h_{lt}, have non-zero values at a critical heat flux point. The vapor generation rate is also determined in the same method which is used for the nucleate boiling heat transfer regime.

2.2.6 Transition Boiling

The transition boiling region of a boiling curve is bounded by the critical heat flux temperature and the minimum film boiling temperature. Transition boiling is characterized by a combination of an unstable film boiling and an unstable nucleate boiling, alternatively existing on a heated surface. Due to its unstable heat transfer characteristics, the physical mechanism governing a transition boiling heat transfer is not fully understood yet. It would be premature for a mechanistic model to be used in safety analysis codes. Instead of a mechanistic model, most existing safety analysis codes utilize simplified correlations which take into account the heat flux contribution by a nucleate boiling and by a film boiling with an appropriate weighting function.

The transition boiling heat transfer model of the RELAP5/MOD3.3 code is based on Chen's transition boiling model [16,17]. It considers the total transition boiling heat transfer to be the sum of a wall heat transfer to a liquid and to a vapor. In the code, the heat flux term to the liquid is substituted with a critical heat flux at a computational local condition for simplification of the computational process. The COBRA-TF code considers the transition boiling to be composed of both a nucleate boiling heat transfer on a wet wall and a film boiling heat transfer on a dry wall. The fraction of the wetted wall is obtained by a second order interpolation between the critical heat flux and minimum film boiling point multiplied by a void fraction multiplier [18,19]. The minimum film boiling temperature T_{MFB} is specified as the larger of either Henry's correlation or a modified Berenson's correlation. In addition, T_{MFB} is restricted to be between 800°F (426.7°C) and 1200°F (648.9°C).

The TRAC-M code considers the transition boiling heat transfer as a sum of the nucleate boiling and film boiling heat transfer terms, weighted by the fraction of the wetted-wall area. The wetted-wall area fraction is calculated by a second order interpolation of the temperature difference between the critical heat flux and the minimum film boiling points [20,21]. The minimum film boiling temperature, T_{MFB}, is obtained by the Henry's correlation, which uses the homogeneous-nucleation minimum stable film boiling temperature [22]. The TRACE [23] and CATHARE codes use a similar interpolation approach to the TRAC-M codes. A modified form of the wetted-wall area fraction, which includes a void fraction multiplier, is used in the TRACE code. The CATHARE code uses the same wetted-wall area fraction as the TRAC-M code. Both codes use the Groeneveld and Stewart's correlation to obtain T_{MFB} [24]. Table 4 shows a summary of the transition boiling models used for the best-estimate safety analysis codes.

Recently, Elias [25] suggested an improved Chen's transition boiling heat transfer model to facilitate in its implementation in large system codes. Though the Chen's model is used in the RELAP5/MOD3.3 code, the heat flux term to the liquid is substituted with a critical heat flux for computational simplicity. In the Elias' model, the

Table 4. Summary of the Transition Boiling Models used in Existing safety Analysis Codes

Code	Transition boiling model
RELAP5/MOD3.3	Chen's model [16,17] $q''_{TB} = q''_{CHF} \cdot A_f \cdot M_f + h_{wgg} \cdot (T_w - T_g) \cdot (1 - A_f \cdot M_f)$ A_f: fractional wetted-wall area M_f: vertical stratification/level model multiplier
COBRA-TF	Bjornard's model [18,19] $q''_{TB} = \xi \cdot q_{CHF} + q_{FB}$ $\xi = \max(0.2, 1-\alpha) \cdot \left(\frac{T_w - T_{MFB}}{T_{CHF} - T_{MFB}} \right)^2$ T_{MFB} : Max. of Henry's and modified Berenson's correlation 426.7 °C<T_{MFB}<648.9 °C
TRAC-M	Jones's model [20,21] $q''_{TB} = \xi \cdot q''_{CHF} + (1-\xi) \cdot q''_{MFB}$ $\xi = \left(\frac{T_w - T_{MFB}}{T_{CHF} - T_{MFB}} \right)^2$ T_{MFB} : Henry's correlation [22]
TRACE	$q''_{TB} = \xi \cdot q''_{CHF} + (1-\xi) \cdot q''_{MFB}$ [23] $\xi = \sqrt{1-\alpha} \cdot \left(\frac{T_w - T_{MFB}}{T_{CHF} - T_{MFB}} \right)^2$ T_{MFB} : Groeneveld-Stewart's correlation [24]
CATHARE	$q''_{TB} = \xi \cdot q''_{CHF} + (1-\xi) \cdot q''_{MFB}$ $\xi = \left(\frac{T_w - T_{MFB}}{T_{CHF} - T_{MFB}} \right)^2$ T_{MFB} : Groeneveld-Stewart's correlation [24]

heat flux term to the liquid is modeled by considering the mechanism of heat removal by a film of liquid at the wall. In addition, a semi-empirical model by Chen for estimating the liquid contact area fraction is slightly modified to improve its prediction capabilities at low pressures and low qualities.

In literature, numerous attempts have been reported to model the transition boiling heat transfer phenomena. However, there is still no model that is widely accepted. At the present stage, a default transition boiling heat transfer model for the SPACE code has not yet been selected. Instead several candidate models proposed by Chen [16], Bjornard [18], Jones [20], and Elias [25] are coded with a user option in the first version of the SPACE code.

The transition boiling heat flux partitioning was performed to comply with the three-field formulation of the SPACE code. Most transition boiling candidate models interpolate the critical heat flux and the minimum film boiling temperature points. Therefore, the heat fluxes at both points are split into three parts and the appropriate interpolation method is applied for each field to obtain the split heat flux.

$$q''_{TB,k} = \xi \cdot q''_{CHF,k} + (1-\xi) \cdot q''_{FB,k} . \quad (15)$$

where k indicates either l, d, or v for continuous liquid, dispersed droplet, or vapor field, respectively, and ξ indicates a weighting function which depends on the specific model. It is noteworthy that the heat fluxes to the dispersed droplet and vapor fields start to increase from zero at the CHF point to split heat fluxes at the minimum film boiling point.

2.2.7 Minimum Film Boiling Temperature

A transition from a transition boiling and a film boiling region is determined by the minimum film boiling temperature, T_{MFB}, in the SPACE code. Physically, the minimum film boiling temperature separates the high temperature region, where an inefficient film boiling or vapor cooling takes place, from the lower temperature region, where the much more efficient transition boiling occurs. Numerous models and correlations have been reported for the minimum film boiling temperature. Note that T_{MFB} is affected by the system pressure, liquid subcooling, surface material, surface condition, flow rate, additives in the liquid, geometry, droplet volume, and initial hot temperature. However, most system codes use a semi-empirical correlation for an easy implementation in the code.

Through an extensive literature survey, the model proposed by Carbajo [26] has been selected as a default model because this model is based on a broad range of databases and it provides a flexible formulation which can account for the effects of several influential parameters on T_{MFB}.

Table 5. Summary of Minimum Film Boiling Temperature Models in the SPACE Code

Model	Formulation
Henry	$T_{MFB} = T_{HN} + (T_{HN} - T_f)\sqrt{\frac{(k\rho C_p)_f}{(k\rho C_p)_w}}$ $T_{HN} = 705.44 - (4.722\times10^{-2})DP + (2.3907\times10^{-5})DP^2 - (5.8193\times10^{-10})DP^3$ [°F] $DP = 3203.6 - P$ [psi]
Modified Berenson	$T_{MFB} = T_B + 0.42(T_B - T_f)\left\{\sqrt{\frac{(k\rho C_p)_f}{(k\rho C_p)_w}}\cdot\left[\frac{h_{fg}}{C_{pw}(T_B - T_f)}\right]\right\}^{0.6}$ $T_B = T_f + 0.127\frac{\rho_v h_{fg}}{k_v}\cdot\left[\frac{g(\rho_f-\rho_g)}{(\rho_f+\rho_g)}\right]^{2/3}\cdot\left[\frac{\sigma}{g(\rho_f-\rho_g)}\right]^{1/2}\cdot\left[\frac{\mu_v}{g(\rho_f-\rho_g)}\right]^{1/3}$
Groeneveld -Stewart	For $P \le 9\times10^6$ [Pa] $T_{MFB} = 557.85 + 0.0441\times10^{-3}P - 3.72\times10^{-12}P^2 - \max\left(0.0, \frac{10^4 X_{eq}}{2.82 + 0.00122\times10^{-3}P}\right)$ For $P > 9\times10^6$ [Pa] $T_{MFB} = T_{sat} + (T_{MFB,9MPa} - T_{sat})\cdot\frac{P_c - P}{P_c - 9\times10^6}$
Carbajo	$\Delta T_{MFB} = \Delta T_{MFB,ISO}\cdot(1+\beta\cdot\gamma)(1+r\cdot G^s) + a\cdot\Delta T_{sub}$ $\Delta T_{MFB,ISO} = \frac{1.372\times10^6}{T_c^{2.3}}\cdot\left(\frac{T_c - T_{sat}}{\sqrt{\mu_f}}\right)^{1/2}$: isothermal temp. difference $\beta = \sqrt{(k\rho C_p)_f/(k\rho C_p)_w}$: surface condition factor λ : roughness factor (1 ~ 52) $r = 0.1$ $s = 0.4$ $a = \frac{4180}{C_{p,f}}\cdot\frac{h_{fg}}{h_f}\cdot\left\{\left[\frac{(k\rho C_p)_f}{(k\rho C_p)_w}\right]^{1/2}\cdot\frac{h_{fg}}{C_{p,w}\Delta T_{MFB,ISO}}\right\}^{0.1}$

$$\Delta T_{MFB} = \Delta T_{MFB,ISO}\cdot(1+\beta\cdot\gamma)(1+r\cdot G^s) + a\cdot\Delta T_{sub} . \quad (16)$$

where the term $(1+\beta\cdot\gamma)$ accounts for the transient contact between the solid and the liquid. The effect of the mass flow rate G is considered in the term $(1+r\cdot G^s)$. Finally the liquid subcooling effect is taken into consideration by the last term $a\cdot\Delta T_{sub}$.

In addition, some specific models which are used in the existing system codes such as RELAP5/MOD3.3, COBRA-TF, TRAC-M, TRACE, and CATHARE are also implemented as alternative models: Henry's model, a modified Berenson's model, and Groeneveld and Stewart's model. Each model can be activated easily by a user option

in the SPACE code. A summary of the selected minimum film boiling temperature models in the SPACE code is shown in Table 5.

2.2.8 Film Boiling

The film boiling heat transfer region is the area where only a vapor phase is in contact with a heated surface. Two film boiling sub-regions can be defined depending on the void fraction. For high void fraction conditions, a liquid-deficient dispersed flow film boiling (DFFB) is usually encountered. As the void fraction becomes higher, a vapor-phase convective heat transfer is encountered asymptotically. A value of 0.8 or 0.9 is usually accepted as a limit void fraction for the DFFB region. If the void fraction is low, an inverted annular film boiling (IAFB) is encountered. An asymptotic heat transfer is a pool boiling as the void fraction becomes small. A value of 0.6 is usually used as a limit void fraction for the IAFB region.

The DFFB and IAFB have been treated individually in the model development process because each boiling regime reveals different heat transfer mechanisms. In the existing DFFB model, it is assumed that a heat transfer takes place in two steps: (1) from the heated surface to the vapor, and (2) from the vapor to the droplets, whereas the IAFB model should take account of a non-equilibrium in both the liquid and vapor phases, and the interfacial heat and momentum exchange should be properly predicted. To simplify the film boiling prediction process, a film boiling look-up table method was developed by Groeneveld et al. [27]. This approach is similar to the CHF look-up table method and it is based on all the available film boiling data in order to cover a wide range of conditions. A major advantage of this look-up table method is that it can be applied to both the DFFB and IAFB regions without a classification of the film boiling region into sub-regions.

For the SPACE code, the look-up table released in 2004 was used to predict a film boiling heat transfer as a default model. As the film boiling look-up table tabulates the overall heat transfer coefficient including conduction, convection and radiation, the total heat flux from the look-up table was partitioned to three parts as follows:

$$q''_{FB} = (q''_v + q''_{rad,v}) + (q''_l + q''_{rad,l}) + (q''_d + q''_{rad,d}) \quad (17)$$

In the SPACE code, the heat flux to the vapor phase q''_v and the heat flux to the droplet phase q''_d are calculated from a Dittus-Boelter type correlation and Bajorek's model [28], respectively. Three split radiation heat fluxes ($q''_{rad,v}$, $q''_{rad,l}$, $q''_{rad,d}$) are obtained by the radiation model which will be described in the next section. Then the remaining heat flux to the liquid phase q''_l can be calculated by subtracting the other obtained heat fluxes from the total heat flux q''_{FB}.

Whereas all the existing safety analysis codes use separate models depending on whether the film boiling sub-region is a DFFB or an IAFB region, a modified form of a Dittus-Boelter type correlation and a modified Bromley's correlation are used extensively for the DFFB and IAFB regions, respectively. Therefore, a similar approach to the existing safety analysis codes is also implemented as an alternative film boiling heat transfer model for comparison. In this case, the summed heat flux to the liquid and to the dispersed droplet phase is assumed to be obtained by the Bromley's correlation. The heat flux to the droplet phase q''_d is calculated from the Bajorek's model. Then, the heat flux to the liquid phase q''_l is obtained by subtracting q''_d from that by the Bromley's model. The split heat flux to the vapor phase q''_v can be calculated from a Dittus-Boelter type correlation.

2.2.9 Radiation

During the post-CHF heat transfer period, the radiation heat transfer rates from the heat structure to the continuous liquid, dispersed droplet, and vapor phases should be taken into account as the heat structure is expected to be in a very high temperature condition. In the IAFB region, all the radiation heat can be assumed to be transmitted to a liquid phase only, because the vapor film is very thin and the droplet fraction is very low. Therefore, Hammouda's model was selected as a default model for the IAFB region for the SPACE code [29].

$$q''_{rad,l} + q''_{rad,d} = \frac{\sigma(T_w^4 - T_s^4)}{1/\varepsilon_w + 1/(\varepsilon_l\sqrt{1-\alpha}) - 1} \quad (18)$$

$$q''_{rad,v} = 0.0 \quad (19)$$

where the radiation heat flux to the liquid phase (Eq. (18)) is assumed to include the heat flux to the droplet phase to avoid numerical discontinuity though the droplet fraction is expected to be close to zero.

On the other hand, most of the radiation heat is transmitted to a droplet as well as a vapor phase in the DFFB region because the liquid fraction is very low. In this case, Sun's model is selected as a default model for the DFFB region [30].

$$q''_{rad,l} + q''_{rad,d} = F_{wd}\sigma(T_w^4 - T_d^4) \quad (20)$$

$$q''_{rad,v} = F_{wv}\sigma(T_w^4 - T_v^4) \quad (21)$$

where the radiation heat flux to the droplet phase (Eq. (20))

is assumed to include the heat flux to the liquid phase even though the liquid fraction is expected to be close to zero. The grey-body factor F_{wd} is a function of the droplet diameter as well as the droplet number density; so, the droplet fraction is replaced with the total liquid fraction.

In the SPACE code, the IAFB region is assumed to exist for the void fraction less than 0.6 and the DFFB region for the void fraction greater than 0.9. These criteria are used widely in the existing safety analysis codes such as COBRA-TF and TRACE. Though the COBRA-TF code uses 0.8 instead of 0.9 as a low limit of the DFFB region, the present limit of 0.9 is considered acceptable as an interpolation method is implemented for a void fraction between 0.6 and 0.9.

A heat flux partitioning between a droplet and a liquid phase is performed by a weighting factor with a relative ratio of the droplet and liquid fraction.

- IAFB region (α<0.6)

$$q''_{rad,d} = q''_{rad,l\_hammouda} \cdot \frac{\alpha_d}{\alpha_l + \alpha_d} \quad \text{wall-to-droplet} \qquad (22)$$

$$q''_{rad,l} = q''_{rad,l\_hammouda} \cdot \frac{\alpha_l}{\alpha_l + \alpha_d} \quad \text{wall-to-liquid} \qquad (23)$$

$$q''_{rad,v} = 0.0 \quad \text{wall-to-vapor} \qquad (24)$$

- DFFB region (α>0.9)

$$q''_{rad,d} = q''_{rad,d\_sun} \cdot \frac{\alpha_d}{\alpha_l + \alpha_d} \quad \text{wall-to-droplet} \qquad (25)$$

$$q''_{rad,l} = q''_{rad,d\_sun} \cdot \frac{\alpha_l}{\alpha_l + \alpha_d} \quad \text{wall-to-liquid} \qquad (26)$$

$$q''_{rad,v} = q''_{rad,v\_sun} \quad \text{wall-to-vapor} \qquad (27)$$

- IADF region (0.6<α<0.9)

$$q''_{rad,d} = \left(\frac{q''_{rad,d\_sun} - q''_{rad,l\_hammouda}}{0.9 - 0.6} \cdot (\alpha - 0.6) + q''_{rad,l\_hammouda} \right) \cdot \frac{\alpha_d}{\alpha_l + \alpha_d} \qquad (28)$$

$$q''_{rad,l} = \left(\frac{q''_{rad,d\_sun} - q''_{rad,l\_hammouda}}{0.9 - 0.6} \cdot (\alpha - 0.6) + q''_{rad,l\_hammouda} \right) \cdot \frac{\alpha_l}{\alpha_l + \alpha_d} \qquad (29)$$

$$q''_{rad,v} = \frac{q''_{rad,v\_sun}}{0.9 - 0.6} \cdot (\alpha - 0.6) \qquad (30)$$

2.2.10 Condensation

Condensation models are incorporated into the wall-to-fluid heat transfer package of the SPACE code. Default and alternative models were selected through an extensive literature survey. As a default model, the same model used in RELAP5/MOD3.3 was selected. For pure steam condensation, a maximum value among the Nusselt's [31], Chato's [32], and Shah's [33] correlations is used in order to consider the geometric and turbulent effects. In the presence of non-condensable gases, the Colburn-Hougen's diffusion model [34] was used. As an alternative model, the non-iterative condensation model proposed by No and Park [35] was selected.

3. CODE IMPLEMENTATION AND VERIFICATION TESTS

3.1 Code Implementation

The programming language for the SPACE code has been selected as C++. Each selected wall-to-fluid heat transfer model has been programmed to a C-function which returns a partitioned heat transfer coefficient and/or a partitioned heat flux. The heat transfer regime selection algorithm was coded in the function "wallheatmode." The major heat transfer models were programmed with the functions of "wallsingle," "wallnucleate," "wallchf," "walltranstion," "wallfilm," and "wallcondensation" according to the heat transfer regime. A CHF and film boiling look-up table was coded into a separate source file for easy maintenance of the SPACE code [36].

3.2 Verification Results

After the developed wall-to-fluid heat transfer package was implemented into the SPACE code, verification work was conducted to identify smoothness between adjacent heat transfer regimes and numerical stability. Two different code verification works were conducted: one is for boiling and the other is for condensation. The wall temperature of the heat structure was arbitrarily increased so that the heat transfer mode was changed from a single phase convection to film boiling, resulting in a typical boiling curve.

Figure 2 shows a typical example of the critical heat flux response surface calculated at 10 MPa where the AECL-LUT method is compared with the Biasi correlation. The Biasi correlation was implemented into the SPACE code as an alternative option. The Biasi correlation shows an exponentially increasing trend in the CHF when the mass flux approaches zero. However, both models result in smooth trends in the application range and a numerical instability was not observed.

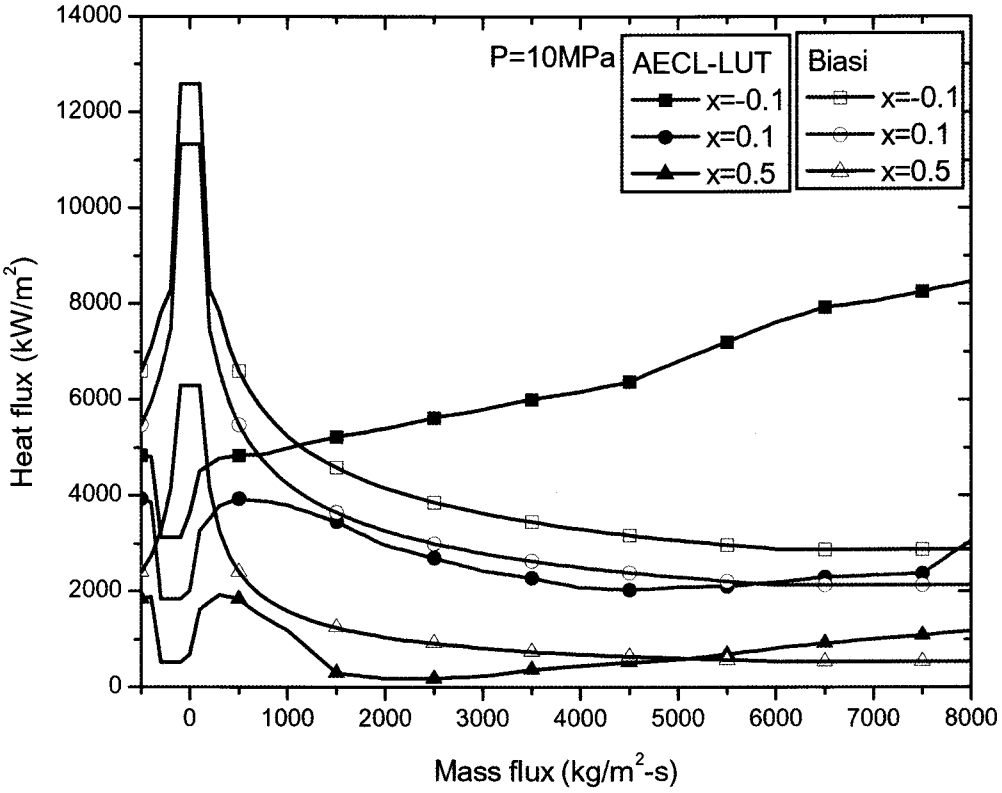

Fig. 2. Comparison of CHF Models at a Pressure of 10.0 MPa

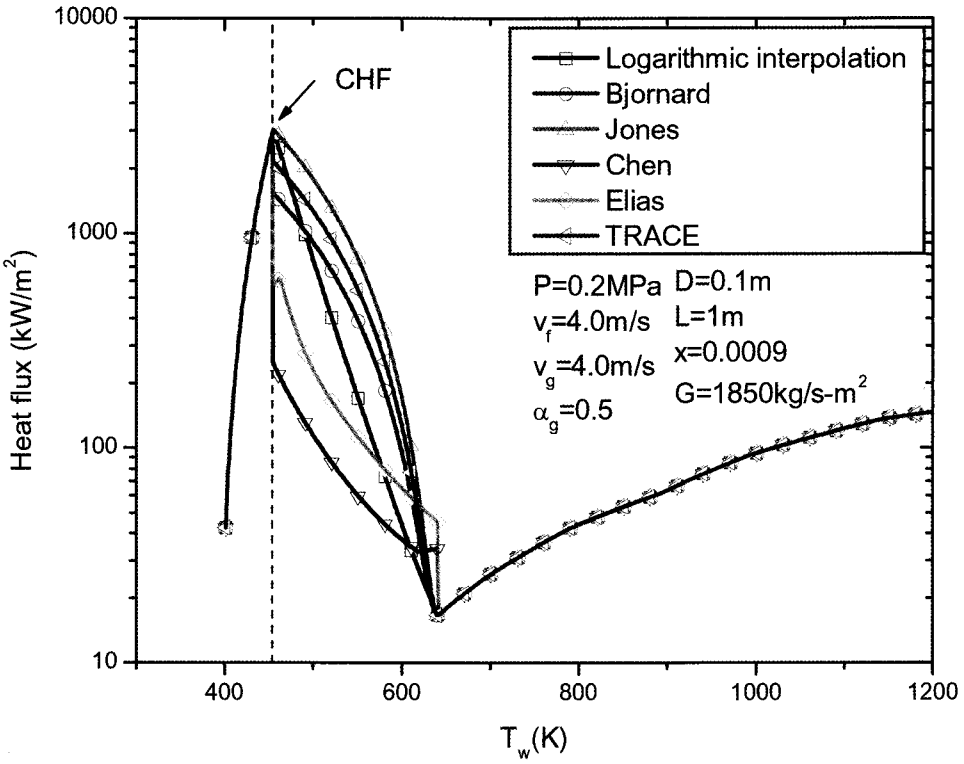

Fig. 3. Effects of Transition Boiling Models on the Boiling Curve

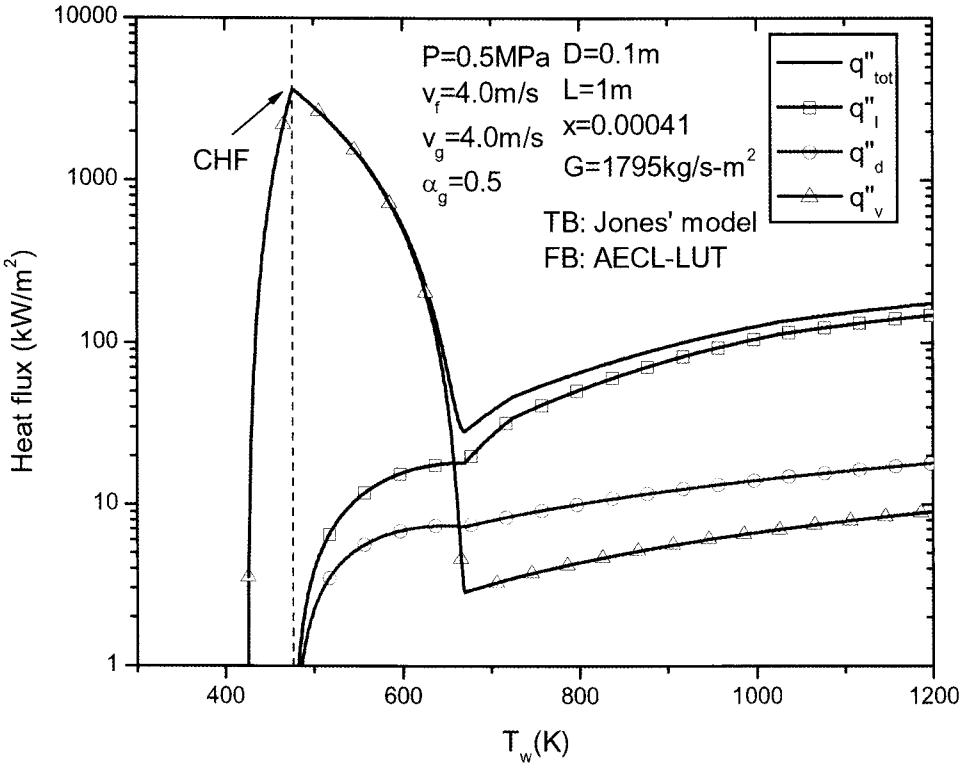

Fig. 4. Split Heat Fluxes of Jones' Model for Transition Boiling and the AECL-LUT Model for Film Boiling

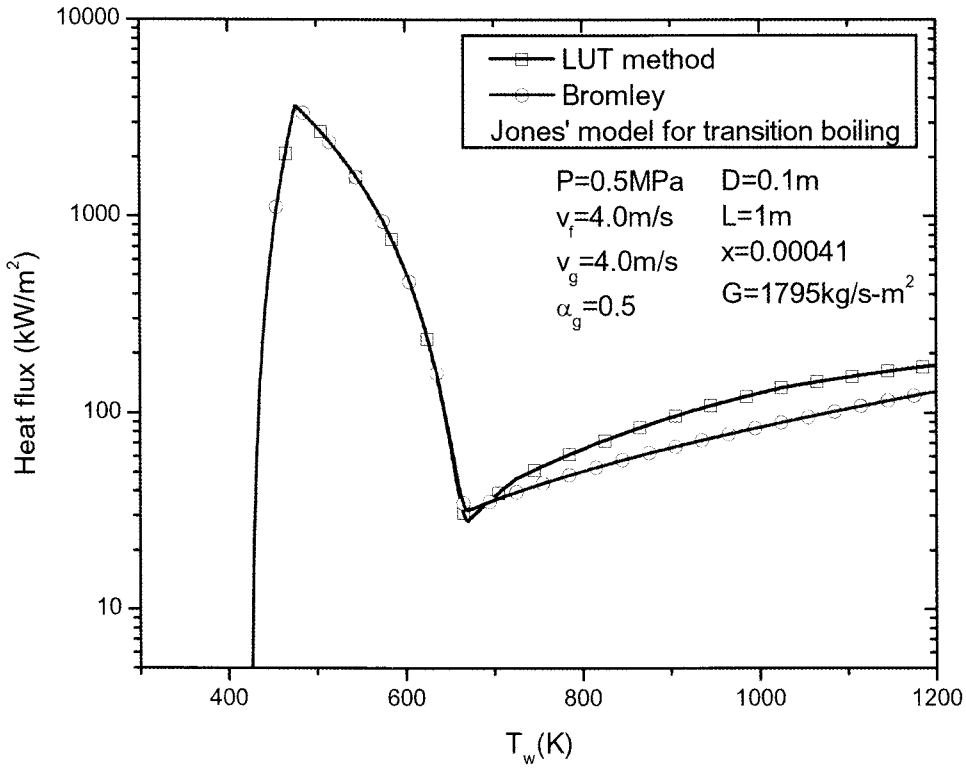

Fig. 5. Comparison of the AECL-LUT Film Boiling Model with Bromley's Model

The effects of several candidate transition boiling models on a boiling curve are shown in Figure 3. Several transition boiling models are compared with one another to investigate their difference and asymptotic trends. A simple logarithmic interpolation method where the wall heat flux is calculated by a straight line in log-log coordinates for connecting the CHF and MFB points is also compared in the present assessment.

The Jones' model and the logarithmic interpolation method produce a smooth connection between the CHF and MFB points. The Bjornard model of COBRA-TF shows a rapid decrease in the wall heat flux due to the multiplier of the weighting function. Among the implemented models, Chen's model in RELAP5/MOD3 produces the smallest heat flux. Finally, Elias' model shows a similar trend to Chen's model but it produces a little higher heat flux than Chen's model. The TRACE model shows a rapid decrease in the wall heat flux after the CHF point due to the effects of the void fraction multiplier of the transition boiling weighting factor. The void fraction multiplier of the TRACE code was introduced to prevent a rapid quenching without any physical rationale. It was found that the difference among the implemented models is not so small compared with other heat transfer regions. A rigorous assessment based on experimental data is impossible at the present stage as a reliable coupling of the wall-to-fluid heat transfer package with a hydraulic solver is not complete yet. It is scheduled to be performed in the near future.

Figure 4 shows a typical heat flux partitioning result for the Jones's transition boiling model. It can be seen that the heat flux is partitioned in a smooth manner.

As mentioned in the previous section, a look-up table method and the Bromley model are coded into the SPACE code. Figure 5 shows a comparison of the film boiling heat flux when two models are used. Though the AECL-LUT method shows a little higher heat flux than the Bromley model, the agreement between the two boiling curves is reasonable for the film boiling region.

The condensation model was assessed by comparing the SPACE results and several models in the literature for different wall temperatures as shown in Fig. 6. The implemented models could simulate the heat fluxes in the horizontal, vertical, and turbulent conditions quite reasonably for a pure steam condensation. However, the two-phase flow properties should be given properly to provide more reasonable results for the assessment of condensation with a non-condensable gas present. In particular, No and Park's model should be improved for low temperature conditions and the iteration scheme should be revised to finalize the Colburn and Hougen's model.

4. CONCLUSION

A wall-to-fluid heat transfer package for the SPACE code has been developed by peer review of the models in the existing safety analysis codes and the leading models in the literature. A heat transfer region selection map has been developed according to the non-condensable gas quality, void fraction, degree of subcooling, and wall temperature. A total of 12 heat transfer regions have been

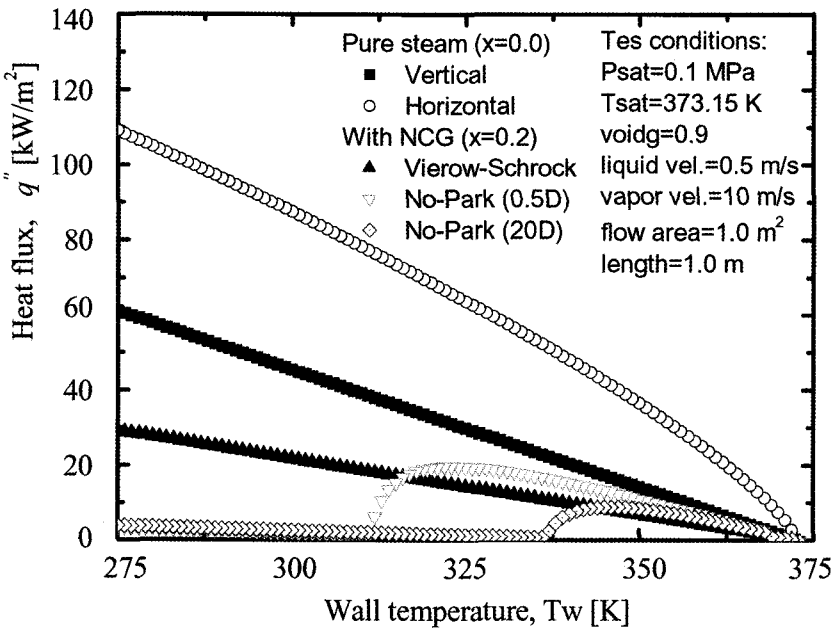

Fig. 6. Heat Fluxes Calculated from the Wall Condensation Models Implemented in the SPACE Code

defined in the heat transfer region selection map. A partitioning methodology which can take into account the split heat flux to continuous liquid, entrained droplet, and vapor fields has been proposed to comply fully with a three-field formulation of the SPACE code.

The developed wall-to-fluid heat transfer package was pre-tested and verified to evaluate the smoothness between two adjacent heat transfer regions. It was found that the present version of the SPACE code produces a continuous boiling curve and a correct asymptotic trend. The implemented condensation models could simulate the heat fluxes reasonably well for the pure steam condition but a few revisions are necessary for assessment of condensation when a non-condensable gas is present.

At the moment, a full assessment for the heat transfer package is not possible because of an incomplete coupling of the adopted hydraulic solver with the developed constitutive equations. More detailed verification work on the developed wall-to-fluid heat transfer package will be carried out when the coupling of a hydraulic solver with the constitutive equations is brought to completion.

ACKNOWLEDGMENTS

This work has been carried out under the support from the Project of Power Industry Research and Development Fund given by the Ministry of Knowledge Economy (MKE) of the Korean government. Additional thanks should also be given to KHNP, the leading company of the Project.

REFERENCES

[1] S. Nukiyama, "Maximum and Minimum Values of Heat Transmitted from Metal to Boiling Water Under Atmospheric Pressure," *Journal of the Japanese Society of Mechanical Engineers*, **37**, p.367 (1934).

[2] Kim, H. D. et al., "Investigation and Selection of Wall-to-Fluid Heat Transfer Correlations for the Development of Constitutive Relation," SPACE's Software Design Description, S06NX08-A-1-RD-03, Rev.00. (2008).

[3] McAdams, W. H., Heat Transmission, 3rd Edition, McGraw-Hill, New York (1954).

[4] Warner, C. Y. and Arpaci, V.S., "An experimental Investigation of Turbulent Natural Circulation in Air at Low Pressure along a Vertical Heated Flat Plate," *Int. J. Heat Mass Transfer*, **11**, p.397 (1968).

[5] Dittus, F. W. and Boelter, L.M.K., "Heat Transfer in Automobile Radiators of the Tubular Type," Publications in Engineering, 2, Univ. of California, Berkeley, p.443 (1930).

[6] Gnielinski, V., "New Equations for Heat and Mass Transfer in Turbulent Pipe and Channel Flow," *Int. Chem. Eng.* **16**, p.359 (1976).

[7] Sellars, J. R., Tribus, M. and Klein, J. S., "Heat Transfer to Laminar Flows in a Round Tube or Flat Conduit: The Graetz Problem Extended," *Transaction of the ASME*, **78**, p.441 (1956).

[8] Lahey, R. T., "A Mechanistic Subcooled Model," *6th Int. Heat Transfer Conf., Toronto, Canada*, **1**, p.293 (1978).

[9] Saha, P. and Zuber, N, "Point of Net Vapor Generation and Vapor Void Fraction in Subcooled Boiling," *Proc. 5th Int. Heat Transfer Conf.*, Toyko, Japan, Paper B4.7 (1974).

[10] Ha, K.S., "Development of the Subcooled Boiling Model using a Computer Tool with the Drift-Flux Model," Master thesis, KAIST (2004).

[11] Chen, J. C., "A Correlation for Boiling Heat Transfer to Saturated Fluid in Convective Flow," ASMS paper, 63-HT-34, p.1 (1963).

[12] Groeneveld, D. C., Cheng, S.C., and Doan, T., "1986 AECL-UO Critical Heat Flux Lookup Table," *Heat Transfer Engineering*, 7, p.46 (1986).

[13] Biasi, L., Clerici, G.C., Garribba, S., Sala, R. and Tozzi,A., "Studies on Burnout, Part 3: A New Correlation for Round Ducts and Uniform Heating and Its Comparison with World Data," *Energia Nucleare*, **14**, p.530 (1967).

[14] Groeneveld, D. C. et al., "The 2006 CHF Lookup Table," *Nuclear Engineering and Design*, **237**, p.1909 (2007).

[15] Groeneveld, D. C. et al., "Lookup Tables for Predicting CHF and Film Boiling Heat Transfer: Past, Present, and Future," *Nuclear Technology*, **152**, p.87 (2005).

[16] Chen, J.C. et al., "A Phenomenological Correlation for Post-CHF Heat Transfer, " NUREG-0237 (1977).

[17] "RELAP5-3D Code Manual Volume IV: Models and Correlation," INEEL-EXT-98-000834, Volume IV, Rev.2.4, (2005).

[18] Bjornard, T.A. and Griffith, P., "PWR Blowdown Heat Transfer," Thermal and Hydraulic Aspects of Nuclear Reactor Safety, ASME, New York, **1**, p.17 (1977).

[19] Thurgood, M. J. et al., "COBRA/TRAC-A Thermal-Hydraulics Code for Transient Analysis of Nuclear Reactor Vessels and Primary Coolant Systems," NUREG/CR-3046 (1983).

[20] Jones, O.C. Jr. and Bankoff, S.G.., "Thermal and Hydraulic Aspects of Nuclear Reactor Safety," ASME, New York, 1, (1977).

[21] Spore, J.W. et al., "TRAC-M/FORTRAN 90 (version 3.0) Theory Manual, " LA-UR-00-910, (2000).

[22] Henry, R.E., "A Correlation for the Minimum Film Boiling Temperature," *AIChE Symposium Series*, **138**, p.81 (1974)

[23] US-NRC, "TRACE V5.0, Theory Manual, Field Equations, Solution Methods, and Physical Models,"

[24] Groeneveld, D.C. and Stewart, J.C., "The Minimum Film Boiling Temperature for Water during Film Boiling Collapse," *Proc. 7th Int. Heat Transfer Conf. Munchen*, **4**, FB37, p393 (1982)

[25] Elias, E. et al., "Development and Validation of a Transition Boiling Model for RELAP5/MOD3 Reflood Simulation," *Nuclear Engineering and Design*, **183**, p.269 (1998).

[26] Carbajo, Juan J., "A Study on the Rewetting Temperature," *Nuclear Engineering and Design*, **84**, p.21 (1985).

[27] Groeneveld et al., "A Look-up Table for Fully Developed Film Boiling Heat Transfer," *Nuclear Engineering and Design*, **225**, p.83 (2003).

[28] Bajorek, S. M. and Young, M. Y., "Direct-Contact Heat Transfer Model for Dispersed-Flow Film Boiling," *Nuclear Technology*, **132**, p.375 (2000).

[29] Hammouda, N., Groeneveld, D.C., and Cheng, S.C., "Two-Fluid Modelling of Inverted Annular Film Boiling," *Int. J. Heat Mass Transfer*, **40**, p.2655 (1997).

[30] Sun, K.H., Gonxalez-Santalo, J.M., and Tien, C.L.,

"Calculations of Combined Radiation and Convection Heat Transfer in Rod Bundles under Emergency Cooling Conditions," *J. of Heat Transfer*, p.414 (1976).
[31] Nusselt, W. A., "The Surface Condensation of Water Vapor", *Zieschrift Ver. Deut. Ing.*, **60**, p.541 (1916).
[32] Chato, J. C., "Laminar Condensation inside Horizontal and Inclined Tubes," *American society of heating, refrigeration and air conditioning engineering journal*, **4**, p.52 (1962).
[33] Shah, M. M., "A general correlation for heat transfer during film condensation inside pipes," *Int. J. Heat Mass Transfer*, **22**, p.547 (1979).
[34] Colburn, A. P. and Hougen, O. A., "Design of cooler condensers for mixtures of vapors with non-condensing gases," *Industrial and Engineering Chemistry*, **26** (1934).
[35] No, H.C. and Park, H. S., "Non-iterative Condensation Modeling for Steam Condensation with Non-condensable Gas in a Vertical Tube," *Int. J. of Heat and Mass Transfer*, **45**, p.845 (2002).
[36] Kim, H. D. et al., "Coding of Wall-to-Fluid Heat Transfer Correlations for the Development of Program Module," SPACE's Software Design Description, S06NX08-A-1-RD-11, Rev.00. (2008).